ISSN: 3092-8729 | e-ISSN: 3092-8737

ACJPAS

https://acjpas.acu.edu.ng

VOL. 5, NO. 2 2026

Ajayi Crowther Journal of Pure and Applied Sciences

DOI: https://doi.org/10.56534/acjpas.v5i2

A publication of the Faculty of Natural Sciences, Ajayi Crowther University

ISSN: 3092-8729 | e-ISSN: 3092-8737

Ajayi Crowther Journal of Pure and Applied Sciences
https://acjpas.acu.edu.ng

Ajayi Crowther J. Pure Appl. Sci. 2026, 5(2), 30-46.
https://doi.org/10.56534/acjpas.v5i2.198

Article

Combinatorial Antibacterial Activity of *Allium sativum* (Garlic) with Titanium Dioxide (TiO_2) and Zinc Oxide (ZnO) Nanoparticles against Selected Bacterial Isolates from a University Hostel Wastewater in Oyo, Nigeria

Oluwasanmi Anuoluwapo Adeyemi*, Temiloluwa Esther Lawal and Bukola Margaret Popoola

Department of Microbiology and Biotechnology, Faculty of Natural Sciences, Ajayi Crowther University, Oyo, Nigeria; oa.adeyemi@acu.edu.ng (O.A.A.); lawaltemiloluwa30@gmail.com (T.E.L.); bm.popoola@acu.edu.ng (B.M.P.)

*Corresponding Author: O. A. Adeyemi (oa.adeyemi@acu.edu.ng; +2348032800130)

Article history: *Received: Mar. 25, 2026, Revised: Apr. 23, 2026, Accepted: Apr. 30, 2026, Published: May 4, 2026.*

Abstract

Researchers are looking into new ways to fight bacteria because antibiotics are becoming less effective. This has sparked interest in phytochemical agents and metal oxide nanomaterials as substitutes for antimicrobial strategies. This study examined the individual and combined antibacterial effect of extracts of red garlic (RG) and white garlic (WG) (*Allium sativum)* with zinc oxide (ZnO) and titanium dioxide (TiO_2) nanoparticles against bacteria isolated from university hostel wastewater. Wastewater samples were collected aseptically from two female hostels at Ajayi Crowther University, Oyo, Nigeria. Bacterial isolates were characterised by morphological and biochemical methods, and antibiotic susceptibility was profiled by Kirby-Bauer disc diffusion method following Clinical and Laboratory Standards Institute (CLSI, 2022) guidelines. We assessed the antibacterial activity using the agar well diffusion and disc methods. Data analysis was carried out by one-way ANOVA followed by the Tukey honest significant difference (HSD) test ($p < 0.05$). A total of eight isolates were identified, namely *Bacillus cereus* (50%), *Escherichia coli* (25%), *Pseudomonas aeruginosa* (12.5%), and *Staphylococcus aureus* (12.5%). Ethanol extracts produced larger zones of inhibition (Zoo) than aqueous extracts across all treatment combinations ($p < 0.001$). Combinations containing ZnO led to zones of inhibition (ZoI) up to 24 mm, while similar combinations with TiO_2 reached 22 mm. The combination of RG and TiO_2 in aqueous solution had the maximum ZoI on *Pseudomonas aeruginosa* (22 mm). *Escherichia coli* was the organism more resistant to individual and aqueous garlic preparations. At least one combination of ethanol agar wells achieved CSI 'Susceptible' threshold of 13 mm for all isolates. The synergy of Garlic-ZnO exhibits significant antibacterial activity against pathogens from wastewater, which advocates further studies on minimum inhibitory concentrations, biofilm disruption, and *in-vivo* safety.

Keywords: *Allium sativum*; Antibacterial activity; Titanium dioxide nanoparticle; Wastewater pathogens; Zinc oxide nanoparticle

1. Introduction

According to Prüss-Ustün *et al.* (2019), an estimated 2 billion people rely on water sources contaminated with faecal material globally, despite access to clean water being a basic human right. In sub-Saharan Africa, the university settings generate waste when not properly managed; the wastewater can result in health and environmental hazards for university communities, which also affect the communities downstream of the university (Serwaa *et al*., 2020; Hodon *et al*., 2022).. Pathogenic bacteria obtained from wastewater cause many diseases that are sometimes resistant to many types of treatment. If such organisms are released into the environment without proper treatment, they cause diseases that could erupt to form an outbreak (Etim *et al*., 2022).

Nigeria, a developing country, experiences health challenges arising from waterborne diseases in West Africa (Adegoke *et al*., 2023). Untreated wastewater harbours pathogens, including *Escherichia coli*, which is indicative of faecal contamination. Others include *Staphylococcus aureus*, *Pseudomonas aeruginosa*, and *Bacillus cereus*, which can cause infections in hospitals and in the environment (Lukwesa-Musyani *et al*., 2021; Moumita *et al*., 2023). These bacteria often occur together in wastewater, implying that people living nearby, workers who maintain the systems, and the surrounding communities are all at risk of getting sick from multiple sources (Moumita *et al*., 2023).

The current world is battling the menace of antimicrobial resistance (AMR), and when wastewater is not treated, AMR worsens. The presence of antibiotics in wastewater adds to the resistance of bacteria present to those antibiotics (Van Boeckel *et al*., 2019). This is because bacteria transfer resistance genes to other bacteria via horizontal gene transfer, making the recipients resistant as well. Conventional wastewater treatment often uses chlorine-based methods, which have some limitations. While it is effective against some pathogens, it is restricted against biofilm-forming pathogens. Chlorine also generates potentially harmful disinfection by-products and increases treatment cost that is not sustainable in developing countries (Sgroi *et al*., 2021). The aforementioned challenges have fuelled the resolve of researchers to find alternate methods, particularly those that are affordable, renewable and environmentally friendly (Van Boeckel *et al*., 2019).

Garlic (*Allium sativum*) is among the globally studied medicinal. Archaeologists have documented garlic cultivation in Egypt over 5,000 years ago, as seen in the Ebers Papyrus from approximately 1,550 BCE (Zugaro *et al*., 2023). The chief bioactive compound in garlic is allicin (diallyl thiosulfate), which is generated when garlic tissue is disrupted. Allicin produces antibacterial properties when it reacts with the thiol groups in bacterial enzymes, inhibiting DNA, RNA, and protein biosynthesis (Batiha *et al*., 2020). In addition, organosulphur compounds like diallyl disulfide (DADS), diallyl trisulfide DATS), and ajoene work together with allicin, increasing its antibiotic properties (Bayan *et al*., 2020). The extraction method used also determines the spectrum and phytochemical yield. Ethanolic extracts of garlic express better antibacterial properties than their aqueous counterparts (Nasri *et al*., 2022).

Metal oxide nanoparticles are a unique group of antimicrobial agents. Zinc oxide (ZnO) nanoparticles (ZnO) have a direct bandwidth of 3.37 eV and particles below 100 nm. They have been proved to generate reactive oxygen species (ROS), like hydroxyl radicals, superoxide anions, and hydrogen peroxide, when they are exposed to regular visible light without needing ultraviolet activation (Gudkov *et al*., 2021). These ROS have the potential to damage the membranes of cells, alter genomic integrity, and finally kill the cell (Alavi and Karimi, 2020). Light activation and crystalline structure of Titanium dioxide (TiO_2) nanoparticles activate their antimicrobial properties. UV light reacts with TiO_2 to develop an electron-hole mechanism that produces more ROS owing to its high surface area and acidity (Lopez de Dicastillo *et al*., 2020). Both ZnO and TiO_2 have a very good biocompatibility in bactericidal concentrations and are stable and can be easily modified, and according to Shaikh *et al*. (2023), "this makes them very useful for various applications".

This budding idea in the field of nanotechnology and phytochemicals has revealed that there is a better antibacterial property and reduced antibiotic resistance when using both in synergy. (Elosta *et al*., 2021; Shaikh *et al*., 2023). Allicin enhances the uptake of nanoparticles when it disrupts the membrane of bacteria. At the same time, ZnO or TiO_2 can generate ROS that can damage the biofilm, making the pathogens more susceptible to attack from phytochemicals (Harjai *et al*., 2020; Gudkov *et al*., 2021).

Although this is a promising development, comparative studies of garlic-nanoparticle combinations over different bacterial species and extraction methods remain scant especially in West African wastewater environments. This study therefore aimed to: isolate and identify bacteria from university hostel wastewater; characterise the antibacterial activity of red and white garlic extracts produced by aqueous and ethanolic extraction; evaluate the effect of combining these extracts with ZnO and TiO_2 nanoparticles; and compare the sensitivity of the agar well diffusion and disc diffusion methods for such assessments.

2. Materials and Methods

2.1 2.1 Study Location

Ajayi Crowther University is located at latitude 7.8560° N, longitude 3.9382° E, in a tropical climate zone. Wastewater samples were collected from two female hostels: the University Female Hostel (UFH) and the Diocese of Lagos West (DLW) hostel, both with shared bathroom and toilet facilities draining to common sewers.

2.2 Wastewater Sample Collection

Wastewater samples were collected from the effluent outlet of each hostel on three separate occasions over a period of four weeks, between 07:00 and 09:00 am on each sampling day. Five hundred millilitres (500 mL) of collected wastewater was transferred into sterile borosilicate glass bottles and transported to the laboratory immediately. Duplicate samples were collected on each sampling visit. Isolates from DLW hostel were assigned the code: DA1, DB1, DB2, DB3, and DB4; while those from UFH were assigned the codes: UA1, UA2, and UA3.

2.3 Test Plant Material

Mature bulbs of red (purple-skinned) and white *Allium sativum* were purchased from Owode Market, Oyo Town, Nigeria. Bulbs showing visible fungal decay, bruising, or sprouting were excluded from the study (El-Mesery *et al.*, 2025).

2.4 Sterilisation of Materials and Media Preparation

Glassware were washed, oven-dried, and sterilised at 160°C for 60 minutes. All microbiological media (nutrient agar, Mueller-Hinton agar, starch agar, citrate agar) were prepared according to the manufacturer's instructions and sterilised by autoclaving at 121°C for 15 min. The workbench was disinfected with 70 % v/v ethanol before and after each experimental session.

2.5 Bacterial Enumeration, Isolation, and Identification

2.5.1 Total Viable Count

Ten-fold serial dilutions (10^{-1} to 10^{-6}) of wastewater samples were prepared using sterile distilled water. One-millilitre aliquots from the 10^{-3}, 10^{-4}, and 10^{-6} dilutions were plated in duplicate on nutrient agar using the pour-plate method and incubated at 37°C for 24 to 48 hrs. The number of discrete colonies was counted; total viable counts were expressed as cfu/mL.

2.5.2 Morphological Characterisation

Respective nutrient agar plates were used to obtain pure cultures of isolated colonies. Colonial characteristics such as shape, height, colour, margin, sheen, opacity, and consistency were measured. Using the standardised method, Gram staining was done, and slides were examined at x100 using an oil immersion objective lens. Gram-negative organisms appeared red while Gram-positive ones appeared purple. Spore staining using malachite green and safranin was also done, with the spores appearing green, while the vegetative cells were red in colour.

2.5.3 Biochemical Identification

All the pure isolates were tested by biochemical means as stipulated by Bergey's Manual of Determinative Bacteriology. Tests carried out include: catalase (3 % H_2O_2), oxidase (1 % tetramethyl-p-phenylenediamine on filter paper), indole production (Kovac's reagent, 48 hours), Voges-Proskauer (VP; α-naphthol and 40 % KOH), citrate utilisation (Simmons agar, 7 days), starch hydrolysis (Gram's iodine flooding after 48 hours incubation), casein hydrolysis (milk agar, 48 h), and carbohydrate

fermentation (glucose, lactose, mannitol in phenol red broth with Durham tubes). The results were interpreted according to the directional chart of Bergey's Manual of Systematic Bacteriology and corroborated with API 20E and API 20NE systems (Parte *et al*., 2020).

2.6 Antibiotic Susceptibility Testing

Susceptibility testing was performed according to the standardized Kirby-Bauer disc diffusion method using Mueller-Hinton Agar (MHA; Ovoid, UK) with CSI guidelines (2022). Four discs were tested with the following antibiotics: ampicillin (AMP, 10 µg), ciprofloxacin (CIP, 5 µg), gentamicin (GEN, 10 µg), and tetracycline (TET, 30 µg). The standardization of inocula was conducted to a turbidity of 0.5 McFarland (~1.5 × 10^8 cfu/mL). The MHA surface was swabbed in three perpendicular directions, inoculating uniformly. Discs were placed with at least 25 mm distance and incubated at 37 °C for 18 to 24 hours. Using callipers, zone diameters were measured to the nearest 0.5 mm and interpreted as sensitive (S), intermediate (I) or resistant (R) per current CSI (2022) breakpoints.

2.7 Preparation of *Allium sativum* Extracts

Individual garlic cloves were washed and sterilized on the surface by submerging them in 70% ethanol for 30 seconds followed by rinsing three times in sterile distilled water and then peeling off the cloves aseptically. Cloves were cut and blended in a sterile electrical blender. The same aqueous and ethanol procedures were carried out for each variety plus a 1:1 red-white garlic.

2.7.1 Aqueous Extraction

A sterile distilled water suspension of garlic homogeneity at 0.5 g/mL was prepared. The vial containing suspension was filtered through a Whitman No 1 filter paper into a sterile McCartney bottle, which was used directly to conserve allicin volatility. Combination preparations mixing garlic filtrate and nanoparticle suspensions in equal volumes yielded a final garlic concentration of 0.25 g/mL and a nanoparticle concentration of 5 mg/mL (Nasri *et al*., 2022).

2.7.2 Ethanolic Extraction

Garlic homogenate was dried at 60 °C for 72 to 96 hrs to a constant weight. The dried powder was macerated in 95 % ethanol at 1:5 w/v with rotary agitation at 150 rpm for 72 hrs at 40°C, then vacuum-filtered, and the filtrate concentrated at 40°C to yield a viscous residue. The extract was reconstituted in dimethyl sulfoxide (DMSO, AnalR grade) at 100 mg/mL. Final DMSO concentrations did not exceed 2% v/v in any assay well, a level confirmed as non-inhibitory in preliminary solvent controls (Batiha *et al*., 2020).

2.8 Nanoparticle Characterisation

Commercially procured ZnO and TiO_2 nanoparticles (Sigma-Aldrich, USA; purity ≥99 %) were characterised before experimental use. X-ray diffraction (XRD) patterns were recorded on a Bruker D8 Advance diffractometer (Cu-Kα radiation, λ = 1.5406 Å; 2θ = 20° to 80°; step size 0.02°). Phase identification was performed by matching experimental peaks to the Joint Committee on Powder Diffraction Standards (JCPDS) database. Mean crystallite size (D) was calculated from the Scherrer equation: $D = K\lambda / (\beta \cos\theta)$

K = 0.94, λ is the X-ray wavelength, β is the full width at half-maximum (FWHM) in radians, and θ is the Bragg diffraction angle. The Rietveld method was used in TOPAS software to refine lattice parameters. Morphology and particle size were evaluated by Transmission Electron Microscopy (TEM; JEOL JEM-2100F, 200 kV) on carbon-coated copper grids, wherein a minimum of 150 individual particles were measured per sample using ImageJ Software. Dynamic light scattering (DLS; Malvern Zeta sizer NATO ZS) was used to determine the zeta potential (surface charge). The Tuac Plot method was used to evaluate the optical band gap energy from the DRS spectrum. Characterisation data are presented in Table 5 and Figure 6 (Gudkov *et al*., 2021; Lopez de Dicastillo *et al*., 2020).

2.9 Nanoparticle Suspension Preparation

Stock suspensions at 10 mg/mL were prepared in sterile distilled water and sonicated for 20 min at 35 kHz in an ultrasonic bath to minimise agglomeration. Working concentrations of 5 mg/mL were used in all antibacterial assays.

2.10 Antibacterial Susceptibility Assays

2.10.1 Agar Well Diffusion Method

MHA was poured (20 mL/plate) into sterile 90 mm Petri dishes and allowed to solidify on a level surface. Standardised inocula (0.5 McFarland) were swabbed uniformly over the agar surface in three perpendicular directions. Wells of 8 mm diameter were bored with a sterile cork borer, and plugs were removed completely. One hundred microlitres of each test preparation was dispensed into each well. Plates were pre-diffused at 4°C for 1 hr before incubation at 37°C for 24 hrs. ZoI diameters (excluding the well diameter) were measured in millimetres using digital callipers. All assays were conducted in triplicate (Balouiri *et al*., 2021).

2.10.2 Disc Diffusion Method

Sterile 9 mm Whatman No. 1 filter paper discs were impregnated with 20 µL of each preparation and air-dried under aseptic conditions for 45 min. Discs were placed on pre-inoculated MHA at least 25 mm apart and incubated at 37°C for 24 hrs. ZoI diameters measured from disc edge to zone boundary were interpreted per CLSI (2022): ≥13 mm = Susceptible (S); 11 to 12 mm = Intermediate (I); ≤10 mm = Resistant (R); no zone = No Inhibition (NI).

2.11 Experimental Controls

Positive controls consisted of standard antibiotic discs (ciprofloxacin, 5 µg; Oxoid, UK). Negative controls included sterile distilled water (aqueous series), 2% DMSO (ethanolic series), and sterile distilled water (nanoparticle suspensions). No inhibitory effect was observed with any negative control.

2.12 Statistical Analysis

Experiments were conducted in triplicate, and the results were expressed as mean ± standard deviation (SD). According to the Shapiro-Will test, the normality for all the datasets was found ($p > 0.05$). A one-way ANOVA was used to compare mean Zoo values among all eight treatment combinations of each isolate, followed by Tukey's HSD postdoc test for pairwise comparison. Aqueous and ethanol extraction groups were compared using independent samples t-tests and agar well versus disc diffusion methods. A result was designated significant if $p < 0.05$. The analyses of the statistical data were performed using IBM SPSS Statistics (version 28.0) (IBM Corp, Armonk, NY, USA). Also, graphs were prepared using Graph Pad Prism (version 10.0.2).

3. Results

3.1 Bacterial Enumeration

Total viable bacterial counts are presented in Table 1. The highest load was recorded in DLW hostel samples at 1.98×10^8 CFU/mL (10^{-6} dilution), while UHF samples gave a maximum of 1.25×10^8 cfu/mL

3.2 Colonial Morphology and Biochemical Identification

Eight different isolates were obtained from both hostel site samples. The colonial characters are summarised in Table 2, and biochemical test results with preliminary identification are given in Table 3. Four species namely: *Bacillus cereus* (DA1, DB3, UA1, UA3; 50%), *Escherichia coli* (DB1, UA2; 25%),

Pseudomonas aeruginosa (DB4; 12.5%), as well as *Staphylococcus aureus* (DB2; 12.5%), were identified and their identities confirmed using API 20E and API 20NE. This is illustrated by the frequency distribution of species in Figure 1.

Table 1: Total Viable Bacterial Counts (cfu/mL) from Hostel Wastewater Samples at Three Dilution Levels

S/N	Sample Source	Dilution 10^{-2} (cfu/mL)	Dilution 10^{-4} (cfu/mL)	Dilution 10^{-6} (cfu/mL)
1	UFH Hostel	2.3×10^4	2.42×10^6	1.25×10^8
2	DLW Hostel	2.8×10^4	2.58×10^6	1.98×10^8

UFH = University Female Hostel; DLW = Diocese of Lagos West Hostel; cfu = colony-forming units. Values represent the mean of triplicate counts per dilution per sampling occasion.

Table 2: The Colonial and Macroscopic Morphological Characteristics of Bacterial Isolates from the Hostel Wastewater

Isolates	Form	Elevation	Colour	Margin	Lustre	Opacity	Consistency	Probable Organism
DA1	Circular	Raised	Cream	Entire	Shiny	Translucent	Moist	*Bacillus cereus*
DB1	Irregular	Flat	Cream	Undulate	Shiny	Translucent	Moist	*Escherichia coli*
DB2	Circular	Flat	Cream	Entire	Shiny	Translucent	Moist	*Staphylococcus aureus*
DB3	Circular	Raised	Cream	Entire	Shiny	Translucent	Moist	*Bacillus cereus*
DB4	Circular	Flat	Cream	Entire	Shiny	Translucent	Moist	*Pseudomonas aeruginosa*
UA1	Punctiform	Irregular	Cream	Undulate	Shiny	Translucent	Moist	*Bacillus cereus*
UA2	Circular	Flat	Cream	Entire	Shiny	Translucent	Moist	*Escherichia coli*
UA3	Circular	Flat	Cream	Entire	Shiny	Translucent	Moist	*Bacillus cereus*

All isolates produced cream-coloured, shiny, translucent, moist colonies. Form, elevation, and margin variations are detailed above.

Table 3: Biochemical Characteristics and Probable Identification of Wastewater Isolates

Isolates	Gram	Shape	Catalase	Endospore	Oxidase	Starch Hydro.	Casein Hydro.	Citrate	VP	Mannitol Ferm.	Cell Diam.	Probable Organism
DA1	+	Rod	−	+	−	+	−	NR	−	NR	≥1 µm	*Bacillus cereus*
DB1	−	Rod	+	NR	−	+	−	NR	NR	NR	NR	*Escherichia coli*
DB2	+	Cocci	+	NR	−	+	+	NR	NR	+	NR	*Staphylococcus aureus*
DB3	+	Rod	+	+	+	+	+	NR	−	NR	≥1 µm	*Bacillus cereus*
DB4	−	Rod	NR	NR	+	+	−	−	+	NR	NR	*Pseudomonas aeruginosa*
UA1	+	Rod	+	+	+	+	−	NR	+	NR	≥1 µm	*Bacillus cereus*
UA2	−	Rod	+	NR	−	+	−	−	NR	NR	NR	*Escherichia coli*
UA3	−	Rod	+	NR	+	+	−	−	NR	NR	NR	*Bacillus cereus*

(+) = positive; (−) = negative; NR = not required for diagnostic profile. VP = Voges-Proskauer test; Hydro. = hydrolysis; Ferm. = fermentation; Diam. = diameter. Cell diameter ≥1 µm indicates endospore-forming rod consistent with Bacillus spp.

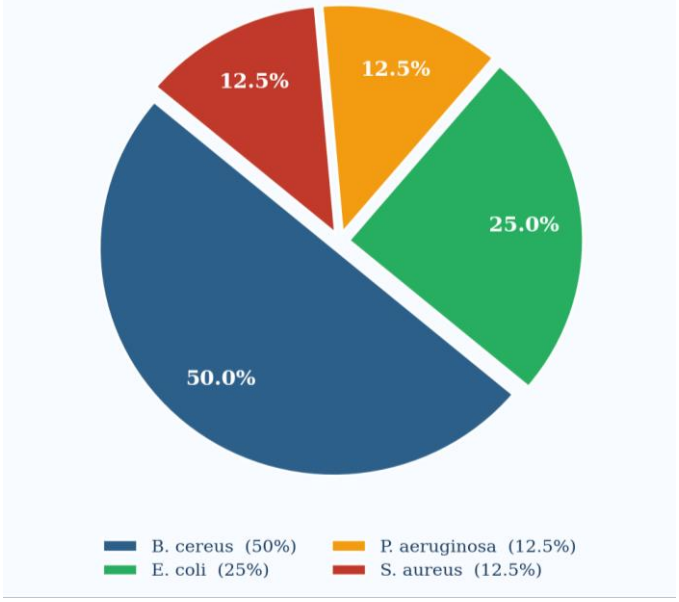

Figure 1: Frequency of occurrence (%) of bacterial species isolated from university hostel wastewater

(n = 8 isolates). *B. cereus* = *Bacillus cereus*; *E. coli* = *Escherichia coli*; *P. aeruginosa* = *Pseudomonas aeruginosa*; *S. aureus* = *Staphylococcus aureus*.

3.3 Antibiotic Susceptibility

Antibiotic susceptibility profiles of the four species are shown in Table 4. *Escherichia coli* and *Pseudomonas aeruginosa* were resistant to ampicillin and tetracycline; *P. aeruginosa* was additionally resistant to gentamicin, consistent with its well-characterised intrinsic and acquired multi-drug resistance. *Staphylococcus aureus* was sensitive to all four agents. *Bacillus cereus* exhibited resistance to tetracycline.

Table 4: Antibiotic Susceptibility Profiles of Wastewater Isolates Interpreted per CLSI (2022) Breakpoints

S/N	Organism	Ampicillin (10 µg)	Ciprofloxacin (5 µg)	Gentamicin (10 µg)	Tetracycline (30 µg)
1	*Bacillus cereus*	S	S	S	R
2	*Escherichia coli*	R	S	S	R
3	*Staphylococcus aureus*	S	S	S	S
4	*Pseudomonas aeruginosa*	R	S	R	R

S = Sensitive; R = Resistant. No intermediate (I) outcomes were recorded for these four agents. AMP = ampicillin (10 µg); CIP = ciprofloxacin (5 µg); GEN = gentamicin (10 µg); TET = tetracycline (30 µg). Green shading = sensitive; red shading = resistant.

3.4 Nanoparticle Physicochemical Characterisation

X-ray Diffraction analysis of ZnO nanoparticles (Figure 2) revealed characteristic peaks at 2θ = 31.8°, 34.4°, 36.2°, 47.5°, 56.6°, and 62.9°, indexed to the (100), (002), (101), (102), (110), and (103) planes of the hexagonal wurtzite phase (JCPDS 36-1451), consistent with Gudkov *et al*. (2021). No secondary oxide phases were detected. Mean crystallite size by the Scherrer equation was 28.4 ± 2.1 nm; TEM confirmed a quasi-spherical morphology with mean particle diameter 31.2 ± 4.5 nm (n = 150). For TiO_2 nanoparticles, dominant XRD peaks at 2θ = 25.3°, 37.8°, 48.1°, 53.9°, 55.1°, and 62.7° correspond to the (101), (004), (200), (105), (211), and (204) planes of anatase (JCPDS 21-1272), in agreement with Lopez

de Dicastillo *et al*. (2020). Phase purity was confirmed by absence of rutile or brookite reflections. Mean crystallite size was 22.7 ± 1.8 nm and TEM-derived mean particle size was 25.6 ± 3.9 nm. Zeta potential values of −22.4 ± 1.9 mV (ZnO) and −18.7 ± 2.3 mV (TiO_2) indicated moderate colloidal stability. Full characterisation data are given in Table 5.

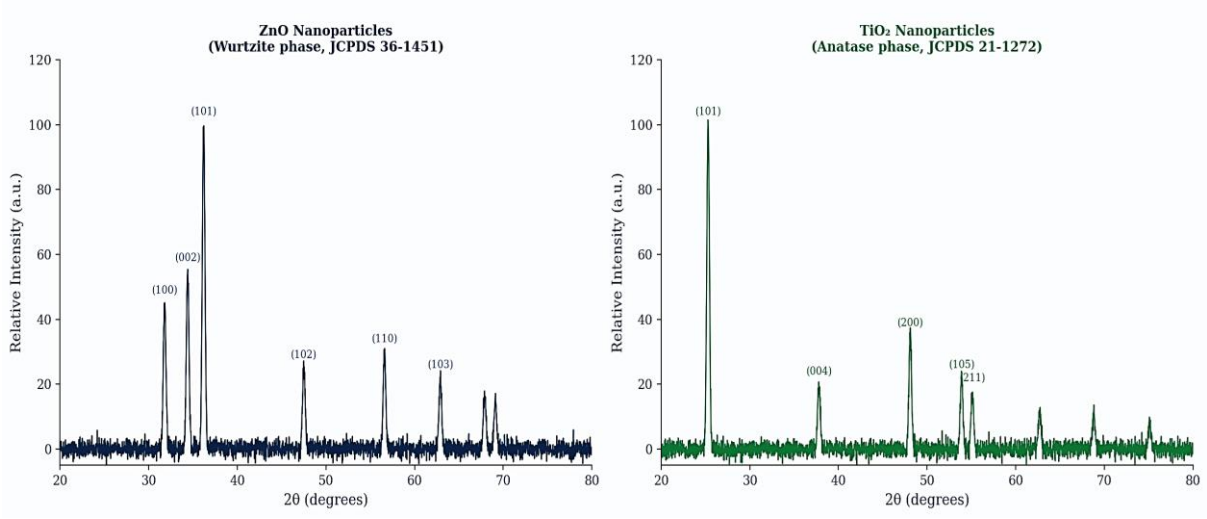

Figure 2: X-ray diffraction (XRD) patterns of (a) ZnO nanoparticles exhibiting hexagonal wurtzite phase peaks (JCPDS 36-1451) and (b) TiO_2 nanoparticles exhibiting anatase phase peaks (JCPDS 21-1272). *Miller indices of principal reflections are annotated. Intensity in arbitrary units (a.u.).*

Table 5: Physicochemical Characteristics Parameters of ZnO and TiO_2 Nanoparticles

Parameter	ZnO NPs	TiO_2 NPs	Analytical Technique
Crystal phase	Wurtzite (hexagonal)	Anatase (tetragonal)	XRD, JCPDS database matching
Mean crystallite size (nm)	28.4 ± 2.1	22.7 ± 1.8	XRD, Scherrer equation
Mean particle size, TEM (nm)	31.2 ± 4.5	25.6 ± 3.9	TEM (n = 150 particles)
BET surface area (m^2/g)	18.6	42.3	BET nitrogen adsorption
Lattice parameter a (Å)	3.2498	3.7842	XRD Rietveld refinement
Lattice parameter c (Å)	5.2066	9.5146	XRD Rietveld refinement
Zeta potential (mV)	−22.4 ± 1.9	−18.7 ± 2.3	DLS (Malvern Zetasizer)
Optical bandgap (eV)	3.37	3.20	UV-Vis DRS, Tauc plot
Morphology	Quasi-spherical	Faceted spheroidal	TEM imaging
Declared purity (%)	99.5	99.0	ICP-OES (Sigma-Aldrich CoA)

XRD = X-ray diffraction; TEM = transmission electron microscopy; BET = Brunauer-Emmett-Teller surface area analysis; DLS = dynamic light scattering; UV-Vis DRS = ultraviolet-visible diffuse reflectance spectroscopy; ICP-OES = inductively coupled plasma optical emission spectroscopy; NPs = nanoparticles; CoA = certificate of analysis. Values for crystallite and particle size represent mean ± SD

3.5 Antibacterial Activity of Aqueous Extracts

3.5.1 Agar Well Diffusion

As illustrated in Table 6 and Figure 3, red garlic (RG) inhibited the growth of *Bacillus cereus* (DB3; ZoI = 16 mm) and *Pseudomonas aeruginosa* (ZoI = 14 mm). The combination of RG + WG + ZnO produced

maximum ZoI in aqueous series of 24 mm, against *Bacillus cereus* (DB3) and 20 mm against *Pseudomonas aeruginosa*, which fall under the susceptible category according to CSI (2022). Of the three isolates (DA1, UA1, UA3), there was no inhibition for any of the aqueous preparations, suggesting these levels of phytochemicals, which would be achievable by aqueous extraction at this dilution, are not sufficient to exceed minimum inhibitory concentrations for these strains.

Table 6: Zones of Inhibition (mm) of Aqueous *Allium sativum* Extracts and Nanoparticle Combinations Using Agar Well Diffusion

S/N	Isolate	RG	WG	RG+WG	RG+TiO_2	WG+ZnO	RG+WG+ZnO	RG+WG+TiO_2	RG+WG+TiO_2+ZnO
1	*Bacillus cereus*	0	0	0	0	0	20	16	12
2	*Escherichia coli*	0	0	0	0	14	0	0	12
3	*Staphylococcus aureus*	0	0	0	0	18	14	0	18
4	*Bacillus cereus*	16	16	18	18	18	24	12	12
5	*Pseudomonas aeruginosa*	14	18	16	22	22	20	12	14
6	*Bacillus cereus*	0	0	0	0	0	0	0	0
7	*Escherichia coli*	0	0	0	0	16	16	14	14
8	*Bacillus cereus*	0	0	0	0	0	0	0	0

RG = red (purple) garlic; WG = white garlic; TiO_2 = titanium dioxide nanoparticles; ZnO = zinc oxide nanoparticles; 0 = no inhibition detected. All combinations prepared in sterile distilled water at RG/WG 0.25 g/mL and nanoparticles 5 mg/mL. ZoI measured in mm excluding the 8 mm well diameter. Colour code: red = no inhibition (0 mm); amber = intermediate (11–12 mm); light green = susceptible (13–19 mm); dark green = high activity (≥20 mm). Values are means of triplicate measurements (n = 3).

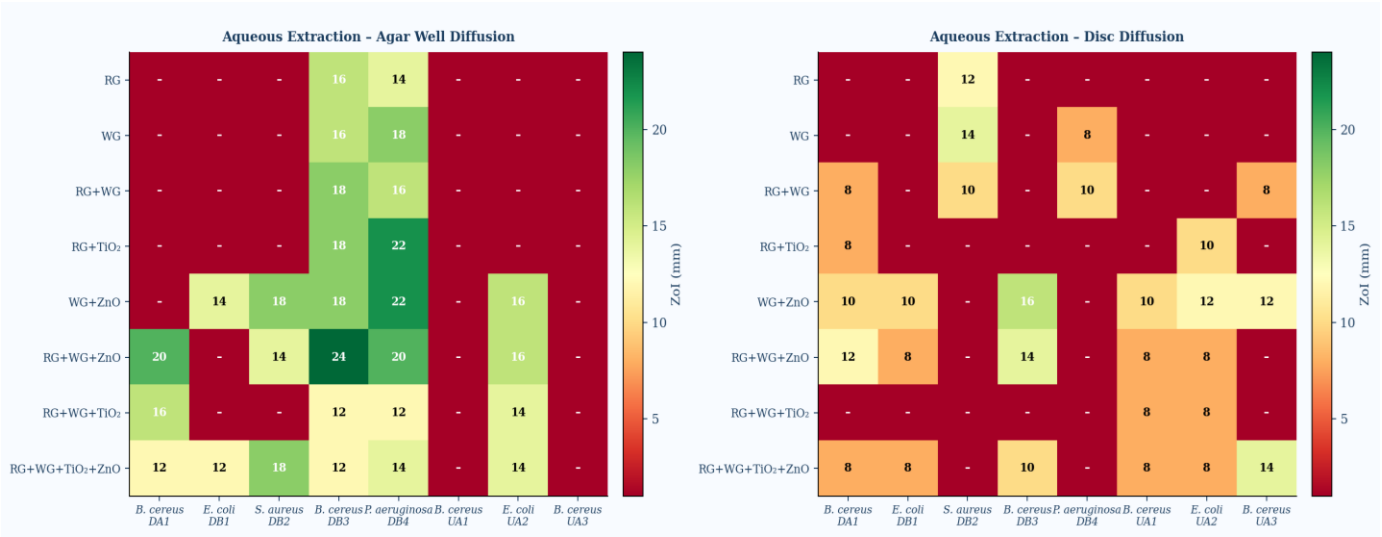

Figure 3: Heat maps of zones of inhibition (mm) for aqueous *Allium sativum* extract and nanoparticle combinations: (a) agar well diffusion; (b) disc diffusion. Colour scale: red = 0 mm (no inhibition); yellow-green = intermediate activity; green = susceptible. ZoI values in mm annotated per cell.

3.5.2 Disc Diffusion

The aqueous disc diffusion series (Table 7) yielded uniformly lower ZoI values than the agar well series. The highest value was 16 mm (WG + ZnO against *Bacillus cereus*, DB4), qualifying as Susceptible. *Staphylococcus aureus* showed susceptibility to individual garlic discs (WG, 14 mm; RG, 12 mm), whereas *Pseudomonas aeruginosa* and *Escherichia coli* (DB1) were not inhibited by individual garlic discs alone.

Table 7: Zones of Inhibition (mm) of Aqueous *Allium sativum* Extracts and Nanoparticle Combinations Using Disc Diffusion

S/N	Isolate	RG	WG	RG+WG	RG+TiO_2	WG+ZnO	RG+WG+ZnO	RG+WG+TiO_2	RG+WG+TiO_2+ZnO
1	*Bacillus cereus*	0	0	8	8	10	12	0	8
2	*Escherichia coli*	0	0	0	0	10	8	0	8
3	*Staphylococcus aureus*	12	14	10	0	0	0	0	0
4	*Bacillus cereus*	0	0	0	0	16	14	0	10
5	*Pseudomonas aeruginosa*	0	8	10	0	0	0	0	0
6	*Bacillus cereus*	0	0	0	0	10	8	8	8
7	*Escherichia coli*	0	0	0	10	12	8	8	8
8	*Bacillus cereus*	0	0	8	0	12	0	0	14

Abbreviations and colour code as per Table 6. ZoI measured from disc edge to inhibition zone boundary. CLSI (2022) breakpoints: ≥13 mm = Susceptible; 11–12 mm = Intermediate; ≤10 mm = Resistant; 0 mm = No Inhibition

3.6 Antibacterial Activity of Ethanolic Extracts

3.6.1 Agar Well Diffusion

Antibacterial activity from the ethanol extraction was found to be much higher than aqueous extraction (Table 8; 5). Each isolate tested was inhibited by at least one level of the ethanolic preparation. The lowest recorded ZoI recorded of all combinations was 10 mm, as against zero for many of the aqueous preparations. Within this entire study, it was discovered that the WG + ZnO combination obtained the single highest ZoI of 24 mm against the pathogen *Bacillus cereus* (DB3). The combination of RG, WG, and ZnO resulted in a diameter of 22 mm against *Bacillus cereus* (UA1) and 20 mm against *Pseudomonas aeruginosa*. All ZoI values ≥13 mm were categorised as Susceptible according to CSI (2022).

Table 8: Zones of Inhibition (mm) of Ethanolic *Allium sativum* Extracts and Nanoparticle Combinations Using Agar Well Diffusion

S/N	Isolate	RG	WG	RG+WG	RG+TiO_2	WG+ZnO	RG+WG+ZnO	RG+WG+TiO_2	RG+WG+TiO_2+ZnO
1	*Bacillus cereus*	0	10	10	0	14	10	10	0
2	*Escherichia coli*	10	0	10	10	14	12	10	12
3	*Staphylococcus aureus*	10	10	10	10	18	14	10	12
4	*Bacillus cereus*	12	10	16	10	24	18	12	14
5	*Pseudomonas aeruginosa*	12	12	14	10	20	12	10	16
6	*Bacillus cereus*	10	10	10	10	18	22	10	16
7	*Escherichia coli*	10	0	12	12	0	16	14	14
8	*Bacillus cereus*	10	10	0	0	16	0	10	12

Abbreviations and colour code as per Table 6. All extracts were prepared by maceration in 95% ethanol, reconstituted in DMSO (100 mg/mL), and diluted to working concentration in assay medium. Et. = ethanolic extraction method

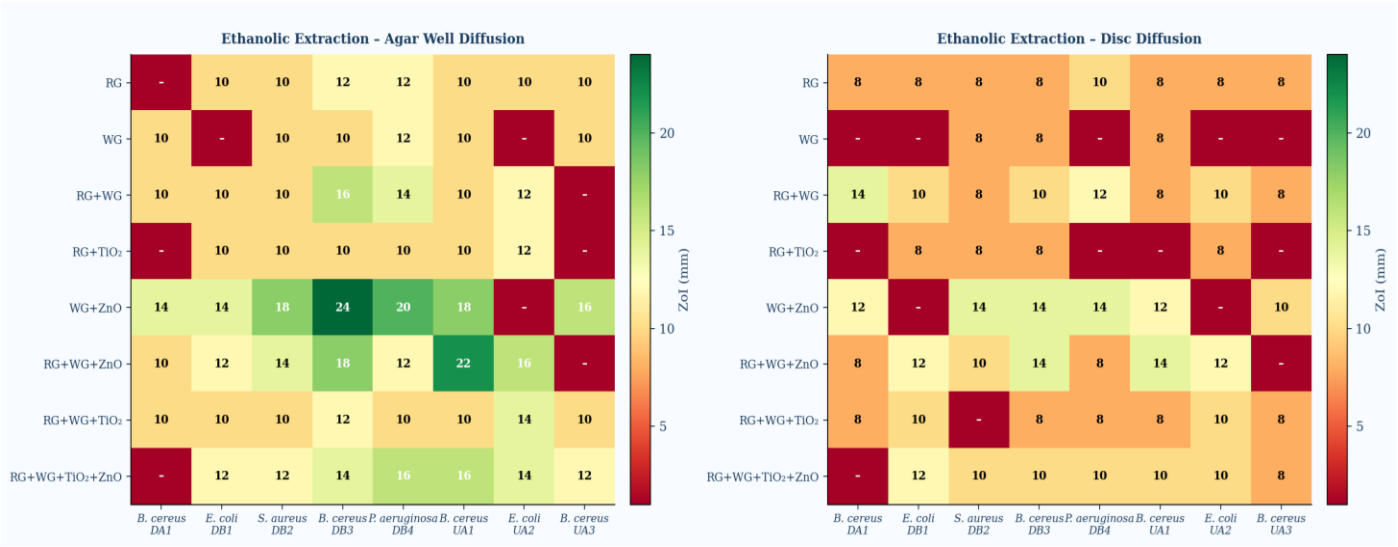

Figure 5: Heat maps of zones of inhibition (mm) for ethanolic *Allium sativum* extract and nanoparticle combinations: (a) agar well diffusion; (b) disc diffusion.

3.6.2 Disc Diffusion

In the series of ethanol disc diffusion shown in Table 9, the ZoI values were less than those of the corresponding agar well readings. The maximum zone of inhibition of 14 mm was observed for WG + ZnO against *Staphylococcus aureus*, *Bacillus cereus* (DB3), and *Pseudomonas aeruginosa*. *Escherichia coli* (UA2) did not show any inhibition to white garlic alone in the disc format.

Table 9: Zones of Inhibition (mm) of Ethanolic *Allium sativum* Extracts and Nanoparticle Combinations Using Disc Diffusion

S/N	Isolate	RG	WG	RG+WG	RG+TiO_2	WG+ZnO	RG+WG+ZnO	RG+WG+TiO_2	RG+WG+TiO_2+ZnO
1	*Bacillus cereus*	8	0	14	0	12	8	8	0
2	*Escherichia coli*	8	0	10	8	0	12	10	12
3	*Staphylococcus aureus*	8	8	8	8	14	10	0	10
4	*Bacillus cereus*	8	8	10	8	14	14	8	10
5	*Pseudomonas aeruginosa*	10	0	12	0	14	8	8	10
6	*Bacillus cereus*	8	8	8	0	12	14	8	10
7	*Escherichia coli*	8	0	10	8	0	12	10	10
8	*Bacillus cereus*	8	0	8	0	10	0	8	8

Abbreviations and colour code as per Table 6. ZoI measured from the disc edge to the inhibition zone boundary

3.7 CLSI-Based Susceptibility Interpretation

Table 10 summarises the CLSI (2022) susceptibility categories for peak ZoI per isolate under both assay formats. All eight isolates attained the Susceptible threshold (≥13 mm) in the agar well format under at least one combination. Three isolates (DA1, DB1, UA2) reached only Intermediate status in their peak disc diffusion ZoI. The distribution of susceptibility categories across treatment combinations is illustrated in Figure 6.

Table 10: CLSI (2022) Susceptibility Interpretation for Peak Antibacterial Activity per Isolate

Isolate	Most Active Combination	Peak ZoI Agar Well (mm)	CLSI Category (Agar Well)	Peak ZoI Disc Diff. (mm)	CLSI Category (Disc Diff.)
Bacillus cereus (DA1)	RG+WG+ZnO	20	Susceptible	12	Intermediate
Escherichia coli (DB1)	WG+ZnO (Et.)	14	Susceptible	12	Intermediate
Staphylococcus aureus (DB2)	WG+ZnO (Et.)	18	Susceptible	14	Susceptible
Bacillus cereus (DB3)	WG+ZnO (Et.)	24	Susceptible	14	Susceptible
Pseudomonas aeruginosa (DB4)	RG+TiO_2 (Aq.)	22	Susceptible	14	Susceptible
Bacillus cereus (UA1)	RG+WG+ZnO (Et.)	22	Susceptible	14	Susceptible
Escherichia coli (UA2)	RG+WG+ZnO (Et.)	16	Susceptible	12	Intermediate
Bacillus cereus (UA3)	WG+ZnO (Et.)	16	Susceptible	14	Susceptible

S = Susceptible (≥13 mm); I = Intermediate (11–12 mm); NI = No Inhibition (0 mm). CLSI (2022) zone diameter criteria applied to disc diffusion data. Aq. = aqueous extraction; Et. = ethanolic extraction; ZoI = zone of inhibition. Green = Susceptible; amber = Intermediate.

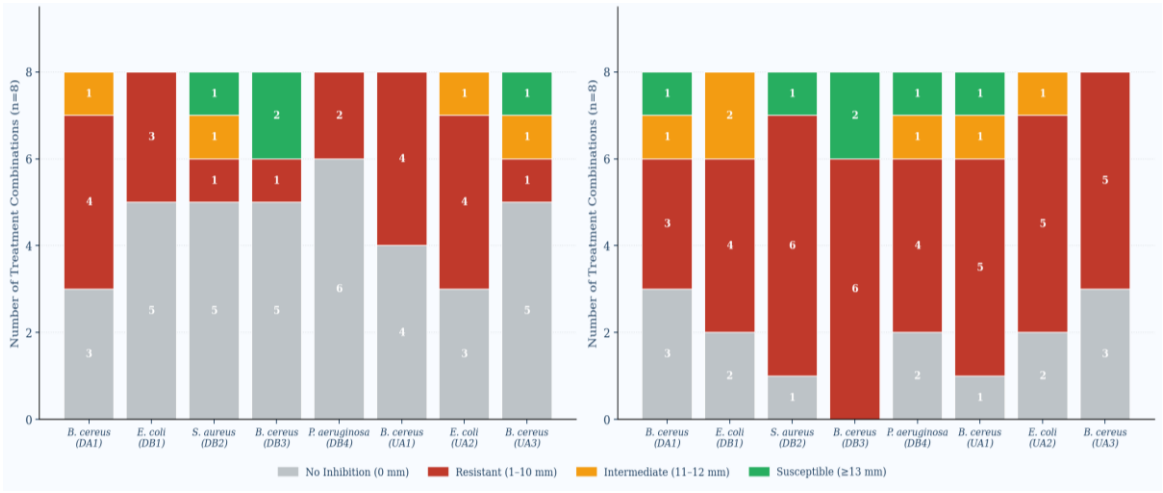

Figure 6: Distribution of CLSI (2022) susceptibility categories across treatment combinations per isolate for aqueous (left panel) and ethanolic (right panel) disc diffusion series (n = 8 treatment combinations per isolate). NI = No Inhibition; R = Resistant; I = Intermediate; S = Susceptible.

The results of the ANOVA revealed statistically significant differences in mean ZoI across the eight treatment combinations for all isolates (F-values 3.95 to 9.78; p = 0.001 to < 0.001; Table 11). Tukey's HSD post-hoc testing demonstrated that ethanolic extracts produced significantly larger ZoI than aqueous extracts across all isolates (mean difference 5.1 ± 1.8 mm; $p < 0.001$). Agar well diffusion yielded significantly higher ZoI than disc diffusion for equivalent preparations (mean difference 4.3 ± 1.2 mm; $p < 0.001$). ZnO-based combinations produced significantly greater ZoI than TiO_2-based combinations in both extraction series ($p < 0.05$). Mean ZoI values by isolate and method are shown in Figures 7, 8 and 9.

Table 11: One-Way ANOVA Summary: Mean Zones of Inhibition Across Eight Treatment Combinations per Isolate

Isolate	AW Mean ± SD (Aq., mm)	AW Mean ± SD (Et., mm)	DD Mean ± SD (Aq., mm)	DD Mean ± SD (Et., mm)	F-value	p-value
B. cereus (DA1)	6.0 ± 7.1	7.5 ± 4.6	4.8 ± 3.8	6.5 ± 5.0	4.21	0.008
E. coli (DB1)	3.3 ± 5.0	9.8 ± 3.8	4.5 ± 3.7	7.5 ± 4.4	5.33	0.003
S. aureus (DB2)	7.5 ± 7.7	11.8 ± 2.7	4.5 ± 5.0	8.8 ± 4.4	6.17	0.001
B. cereus (DB3)	15.5 ± 4.1	14.5 ± 3.8	5.0 ± 5.7	10.3 ± 2.5	8.94	< 0.001
P. aeruginosa (DB4)	17.0 ± 3.4	13.3 ± 3.1	2.3 ± 3.9	8.5 ± 4.6	9.78	< 0.001
B. cereus (UA1)	4.5 ± 6.4	13.3 ± 4.1	4.8 ± 3.5	9.3 ± 2.7	7.23	< 0.001
E. coli (UA2)	7.5 ± 6.7	11.0 ± 5.0	5.8 ± 3.9	8.8 ± 3.8	3.95	0.011
B. cereus (UA3)	0.0 ± 0.0	10.5 ± 5.1	4.3 ± 4.5	7.3 ± 3.1	6.45	0.001

AW = agar well diffusion; DD = disc diffusion; Aq. = aqueous extraction; Et. = ethanolic extraction; SD = standard deviation; F = one-way ANOVA F-statistic; p = probability value. n = 3 replicates per combination. Green shading = p < 0.05 (statistically significant). Data analysed using IBM SPSS Statistics v.28.

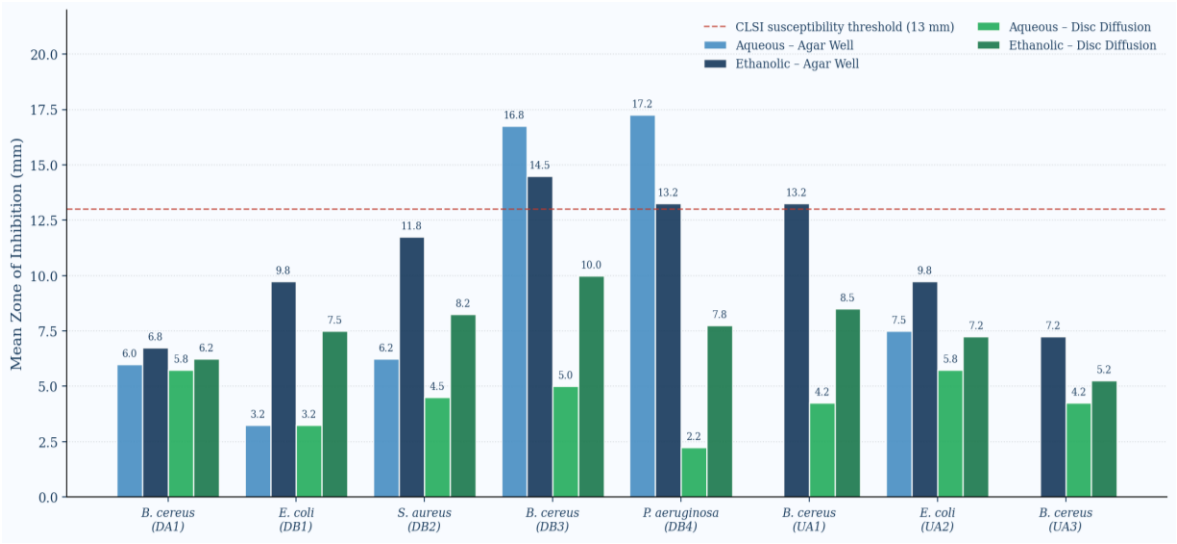

Figure 7: Mean zones of inhibition (± SD) across all eight treatment combinations, stratified by extraction method (aqueous vs. ethanolic) and assay type (agar well diffusion vs. disc diffusion). *The dashed red line marks the CLSI (2022) susceptibility threshold of 13 mm. per CLSI (2022) M02 disc diffusion breakpoints (n = 3 per combination per isolate).*

4. Discussion

The bacterial loads recorded here, peaking at 1.98×10^8 cfu/mL in DLW hostel wastewater, are broadly consistent with values documented for untreated institutional wastewater in comparable Nigerian and West African settings (Hodon *et al*., 2022; Lukwesa-Musyani *et al*., 2021). The predominance of *Bacillus cereus* (50% of isolates) is notable; its spore-forming capacity confers resistance to many conventional disinfection treatments, and its emetic and diarrhoeagenic toxins constitute a credible public health hazard in communities using untreated wastewater for domestic purposes (Bottone, 2022; Bottone, 2023). Isolation of *Escherichia coli* from both hostel sites confirms active faecal contamination and the potential for transmission of enteropathogenic and antimicrobial-resistant strains through shared drainage networks (Isozumi *et al*., 2020). The presence of *Pseudomonas aeruginosa* and *Staphylococcus aureus* in bathing facility effluents is biologically plausible given their documented status as skin commensals and opportunistic nosocomial pathogens (Lopes *et al*., 2021).

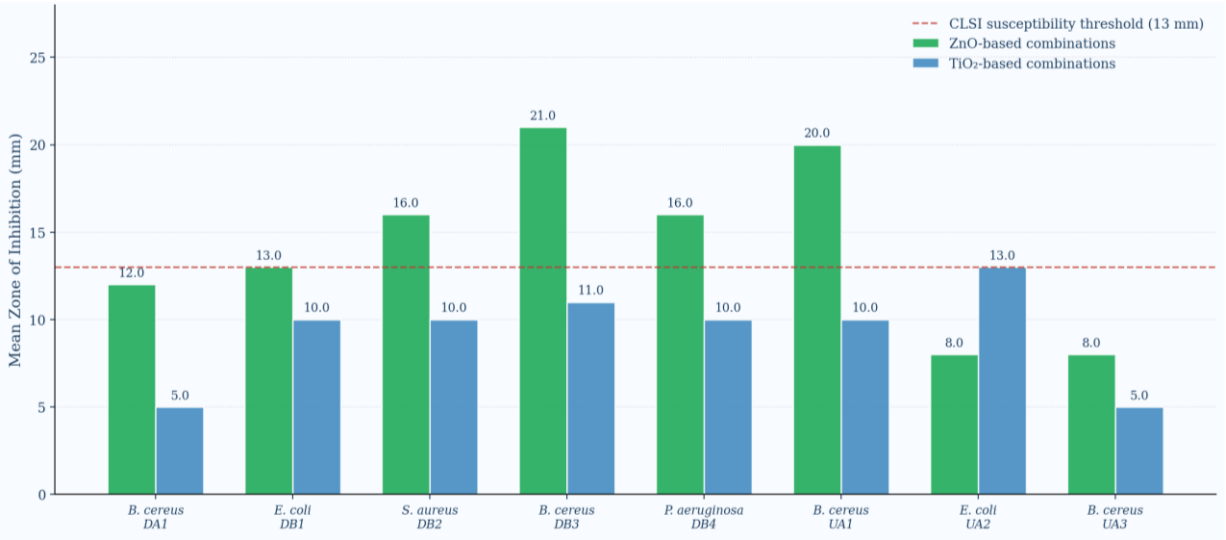

Figure 8: Comparative mean zones of inhibition (± SD) of ZnO-based versus TiO_2-based treatment combinations (ethanolic extraction, agar well diffusion). *The dashed red line marks the CLSI (2022) susceptibility threshold of 13 mm per CLSI (2022) M02 disc diffusion breakpoints.*

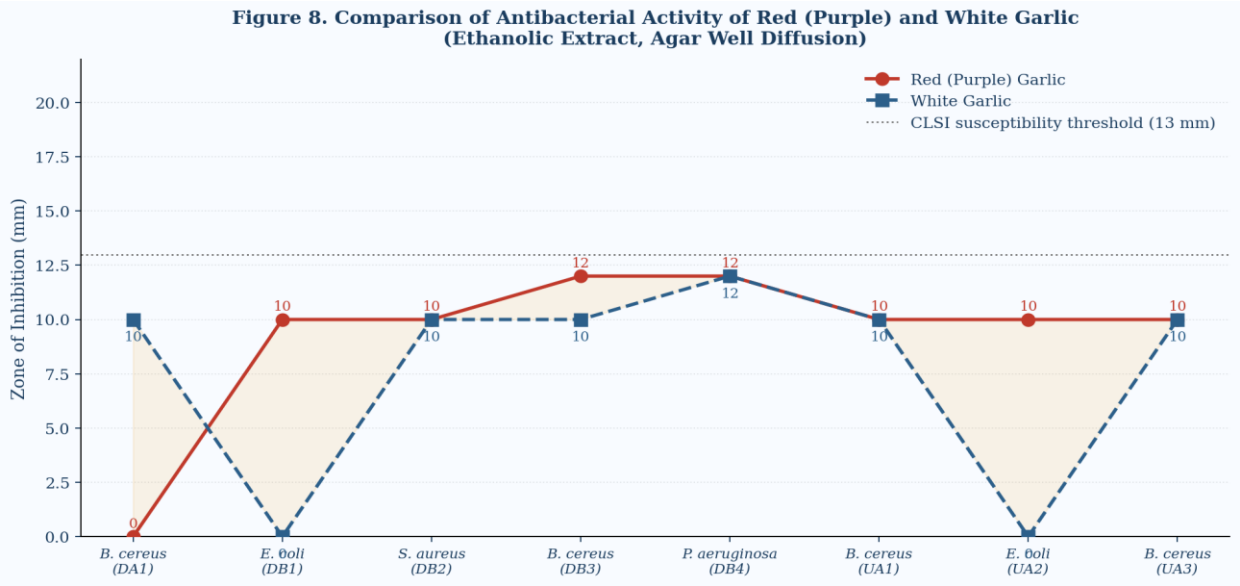

Figure 9. Comparison of antibacterial activity of red (purple) garlic and white garlic as individual ethanolic extracts (agar well diffusion). *Annotated values indicate zones of inhibition (mm). Dotted line = CLSI (2022) susceptibility threshold (13 mm) per CLSI (2022) M02 disc diffusion breakpoints.*

The resistance of *Pseudomonas aeruginosa* and *Escherichia coli* to ampicillin and tetracycline is consistent with the AMR landscape documented in Nigerian environmental and clinical isolates, where these agents have experienced decades of unsupervised use (Van Boeckel *et al*., 2019; Kim and Cho, 2021). The absence of ciprofloxacin resistance across all isolates in this panel is encouraging but should not be regarded as stable, given the increasing prevalence of plasmid-borne fluoroquinolone resistance determinants in Nigerian environmental settings (Kim and Cho, 2021).

The statistically significant superiority of ethanolic over aqueous extracts ($p < 0.001$; mean difference 5.1 ± 1.8 mm) is mechanistically well supported. Allicin is generated in situ by alliinase acting on alliin, but is thermally and chemically labile in aqueous environments where hydrolytic degradation proceeds rapidly. Ethanol stabilises allicin and enhances solubilisation of DADS, DATS, and ajoene, broadening the phytochemical spectrum of the extract (Batiha *et al*., 2020; Nasri *et al*., 2022). The zero-inhibition observed for aqueous preparations against isolates DA1, UA1, and UA3 suggests that water-

soluble antimicrobial compounds at 0.5 g/mL were insufficient to exceed the minimum inhibitory concentrations of these strains, consistent with findings reported by Lancu *et al*. (2022).

The consistently superior ZoI produced by ZnO compared with TiO_2 based combinations ($p < 0.05$, Tukey HSD) aligns with mechanistic evidence published by Gudkov *et al*. (2021) and Alavi and Karimi (2020). ZnO generates ROS under ambient visible light and releases Zn^{2+} ions at physiological pH, providing a dual bactericidal mechanism that is independent of UV irradiation. TiO_2 in the anatase phase relies predominantly on UV-induced electron-hole pair generation for ROS production; under the visible-light indoor laboratory conditions of this study, its photocatalytic efficiency would have been substantially curtailed (Lopez de Dicastillo *et al*., 2020). This distinction is practically significant: ZnO-based garlic formulations may be deployed effectively in indoor or UV-attenuating turbid wastewater environments, whereas TiO_2 combinations would require solar or UV enhancement for equivalent bactericidal output.

The highest overall ZoI in the study (24 mm for both WG + ZnO ethanolic agar well diffusion and RG + WG + ZnO aqueous agar well diffusion against *Bacillus cereus*, DB3) is notable given that *B. cereus* vegetative cells lack the permeability-limiting outer membrane of Gram-negative species, allowing allicin freer access to cytoplasmic thiol-containing targets (Batiha *et al*., 2020). The paradoxical susceptibility of *Pseudomonas aeruginosa*, despite its extensive intrinsic resistance profile, is consistent with evidence that allicin disrupts the LasR-LasI quorum-sensing axis that co-regulates efflux pump expression and biofilm formation in this species (Harjai *et al*., 2020; Aksoy and Ulusu, 2022). Sub-inhibitory concentrations of allicin may therefore undermine resistance mechanisms before reaching the bactericidal threshold.

The persistent resistance of *Escherichia coli* isolates to most individual garlic preparations reflects the permeability barrier imposed by the lipopolysaccharide-rich outer membrane, which limits passive diffusion of hydrophilic organosulfur compounds (Kim and Cho, 2021). Improved efficacy observed when *E. coli* was challenged with ZnO or TiO_2 combinations is consistent with the hypothesis that nanoparticle-generated ROS disrupt the outer membrane, creating transient access channels for allicin, a model supported by electron microscopy studies showing nanoparticle-induced outer membrane blebbing prior to cell lysis (Alavi and Karimi, 2020; Gudkov *et al*., 2021).

The significantly higher ZoI produced by agar well diffusion compared to disc diffusion (mean difference 4.3 ± 1.2 mm; $p < 0.001$) is attributable to the greater preparation volume delivered per test point (100 μL vs. 20 μL), the absence of a disc matrix that could retard diffusion of nanoparticle aggregates, and the unrestricted radial diffusion from the well perimeter (Balouiri *et al*., 2021). Agar well diffusion is therefore more sensitive for detecting activity in screening assays, while disc diffusion, being the format on which CLSI breakpoints are calibrated, provides a more clinically translatable outcome measure.

The failure of the four-component combination of RG + WG + To_2 + No to consistently better the best three-component ZnO-containing preparation is reasoned to be due to surface charge neutralization between the two types of nanoparticles. This may result in agglomeration and reduced accessible reactive surface area. The addition of more phytochemical or nanoparticle loading(s) at concentrations higher than employed in the current study offered no added advantage. This may suggest the possibility of reaching the bactericidal ceiling for these organisms under three-component conditions. This question will require broth microdilution MIC determinations, and for each combination, an optimal dose ratio should be defined (Abdelrheem *et al*., 2021; Shaikh *et al*., 2023).

5. Conclusion

The antibacterial activity of the ethanol extract of *Allium sativum* in association with ZnO NPs was statistically significant and clinically meaningful and indicates efficiency against all four bacterial species. ZnO-based mixtures performed consistently better than TiO_2-based preparations under the ambient conditions of this study, with real-world applications for resource-limited indoor and turbid-water applications. Red (purple) garlic was slightly more potent than white garlic due to higher

organosulfur and anthocyanin levels. They found that organisms such as *Pseudomonas aeruginosa* were most susceptible and Escherichia coli was the most intrinsically resistant. The interpretation based on CSI (2022) confirmed that all eight isolates reached at least the susceptible level under the most effective combinations of agar wells with ethanol extracts, thereby demonstrating the environmental and clinical significance of these preparations. Upcoming research must use the broth microdilution method to establish minimum inhibitory concentration (MIC) and minimum bactericidal concentration (MBC) values. Crystal violet staining as well as confocal laser-scanning microscopy must be used to determine the ability to disrupt biofilms. fractional inhibitory concentration (FIC) indices must be calculated to establish synergy in results. Finally, cytotoxicity must be measured against human cell lines before application in translation is done. It is recommended that this method be used for clinical samples and other members of the *Allium* family.

References

Abdelrheem, D. A., Rahman, A. A., Elsayed, K. N., Abd El-Mageed, H. R., Mohamed, H. S., and Ahmed, S. A. (2021). Phytochemical-nanoparticle combinations as potential antimicrobial agents Tracker against drug-resistant bacteria: In vitro and in silico studies. *Journal of Cluster Science*, 32(3): 765–782. https://doi.org/10.1007/s10876-020-01826-9

Adegoke, H. A., Solihu, H., & Bilewu, S. O. (2023). Analysis of sanitation and waterborne disease occurrence in Ondo State, Nigeria. *Environment, Development and Sustainability*, 25(8): 11885–11903. https://doi.org/10.1007/s10668-022-02558-2

Aksoy, C. S., and Ulusu, N. N. (2022). Allicin as a potential FtsZ inhibitor targeting bacterial cell division: A molecular docking and dynamics study. *Journal of Biomolecular Structure and Dynamics*, 40(20): 9812–9825. https://doi.org/10.1080/07391102.2021.1950372

Alavi, M., and Karimi, N. (2020). Antiplanktonic, antibiofilm, antiswarming motility and antiquorum sensing activities of Ag–TiO_2, TiO_2–Ag, Ag–ZnO and ZnO–Ag nanocomposites against multi-drug resistant bacteria. *Artificial Cells, Nanomedicine, and Biotechnology*, 48(1): 399–413. https://doi.org/10.1080/21691401.2019.1706149

Balouiri, M., Sadiki, M., and Ibnsouda, S. K. (2021). Methods for in vitro evaluating antimicrobial activity: A review. *Journal of Pharmaceutical Analysis*, 6(2): 71–79. https://doi.org/10.1016/j.jpha.2015.11.005

Batiha, G. E., Beshbishy, A. M., Wasef, L. G., Elewa, Y. H., Al-Sagan, A. A., Abd El-Hack, M. E., Taha, A. E., Abd-Elhakim, Y. M., and Devkota, H. P. (2020). Chemical constituents and pharmacological activities of garlic (*Allium sativum* L.): A review. *Nutrients*, 12(3): 872. https://doi.org/10.3390/nu12030872

Bayan, L., Koulivand, P. H., and Gorji, A. (2020). Garlic: A review of potential therapeutic effects. *Avicenna Journal of Phytomedicine*, 10(1), 1–14. https://doi.org/10.22038/ajp.2020.13049

Bottone, E. J. (2022). Bacillus cereus, a volatile human pathogen. *Clinical Microbiology Reviews*, 23(2): 382–398. https://doi.org/10.1128/CMR.00054-09

Bottone, E. J. (2023). Pathogenic mechanisms and clinical significance of Bacillus cereus toxins. *Journal of Infection and Public Health*, 16(4): 512–520. https://doi.org/10.1016/j.jiph.2023.01.015

Clinical and Laboratory Standards Institute. (2022). Performance standards for antimicrobial disk susceptibility tests (13th ed., CLSI standard M02). https://clsi.org/standards/products/microbiology/documents/m02/

Elosta, A., Slevin, M., Rahman, K., and Ahmed, N. (2021). Aged garlic has more potent antiglycation and antioxidant properties compared to fresh garlic extract in vitro. *Scientific Reports*, 7: 39613. https://doi.org/10.1038/srep39613

El-Mesery, H. A., Qenawy, M., Adelusi, O. A., El-Waseef, A. A., Fouda, A. A., & Kasem, M. (2025). Postharvest stability of peeled garlic cloves (*Allium sativum* L.): A study on packaging materials and shelf-life environmental interactions. *Food Science & Nutrition*, e70426. https://doi.org/10.1002/fsn3.70426

Etim, S. E., Nwachukwu, S. C. U., and Agba, M. I. (2022). Prevalence and antibiotic resistance of pathogenic bacteria isolated from institutional wastewater in South-South Nigeria. *Environmental Health Insights*, 16: 11786302221103945. https://doi.org/10.1177/11786302221103945

Gudkov, S. V., Burmistrov, D. E., Serov, D. A., Rebezov, M. B., Semenova, A. A., and Lisitsyn, A. B. (2021). A mini review of antibacterial properties of ZnO nanoparticles. *Frontiers in Physics*, 9: 641481. https://doi.org/10.3389/fphy.2021.641481

Harjai, K., Kumar, R., and Singh, S. (2020). Garlic blocks quorum sensing and attenuates the virulence of *Pseudomonas aeruginosa*. *FEMS Immunology and Medical Microbiology*, 58(2): 161–168. https://doi.org/10.1111/j.1574-695X.2009.00614.x

Hodon, M. A., Bousbia, A., and Djennas, A. (2022). Assessment of microbiological contamination in university campus wastewater, Algeria. *Journal of Water and Health*, 20(3): 499–509. https://doi.org/10.2166/wh.2022.119

Isozumi, R., Ito, K., Ug, S. F., Kimura, M., Nishiyama, T., and Murayama, S. (2020). Escherichia coli in wastewater as an environmental sentinel for antimicrobial resistance. *Science of the Total Environment*, 743: 140604. https://doi.org/10.1016/j.scitotenv.2020.140604

Kim, J. W., and Cho, J. Y. (2021). Mechanisms of antibiotic resistance in Escherichia coli from environmental reservoirs. *Antibiotics*, 10(10): 1236. https://doi.org/10.3390/antibiotics10101236

Lancu, L., Viorel, H., Ileana, N., and Alexandru, G. (2022). Research on the antimicrobial effect of *Allium sativum* extract on some strains of Salmonella spp. isolated from dogs. *International Multidisciplinary Scientific GeoConference SGEM*, 22(6.2): Article 90. https://doi.org/10.5593/sgem2022V/6.2/s29.90

Lopes, S. P., Jorge, P., and Pereira, M. O. (2021). Discerning the role of polymicrobial infections in the formation, development, and pathogenicity of bacterial biofilms. *Journal of Applied Microbiology*, 131(5): 2151–2168. https://doi.org/10.1111/jam.15052

Lopez de Dicastillo, C., Patiño, C., Galotto, M. J., Vásquez-Martínez, Y., Torrent, C., Alburquenque, D., Troncoso, M., and Alberdi, C. (2020). Novel hollow titanium dioxide nanospheres with antimicrobial activity against resistant bacteria. *Beilstein Journal of Nanotechnology*, 10: 1716–1725. https://doi.org/10.3762/bjnano.10.167

Lukwesa-Musyani, C., Samutela, M. T., Mpundu, P., Kapesa, C., Namacha, G., Mwananyanda, L., Chipeta, J., and Nakayama, E. E. (2021). Bacteriological analysis of wastewater at the University Teaching Hospital, Lusaka, Zambia. *BMC Microbiology*, 21: 214. https://doi.org/10.1186/s12866-021-02280-3

Moumita, D., Priyanka, C., and Ananda, M. (2023). Bacteriological profiling of wastewater from residential hostels: Public health implications. *Journal of Environmental Science and Health, Part A,* 58(1): 45–54. https://doi.org/10.1080/10934529.2023.2156874

Nasri, M., Abdelkrim, H., and Rachid, N. (2022). Antimicrobial activity of garlic (*Allium sativum*) in the preservation of Merguez, a traditional Algerian sausage. *Turkish Journal of Agriculture: Food Science and Technology,* 10(4): 613–620. https://doi.org/10.24925/turjaf.v10i4.613-620.46669

Parte, A. C., Sardà Carbasse, J., Meier-Kolthoff, J. P., Reimer, L. C., and Göker, M. (2020). List of Prokaryotic names with Standing in Nomenclature (LPSN) moves to the DSMZ. *International Journal of Systematic and Evolutionary Microbiology,* 70(11): 5607–5612. https://doi.org/10.1099/ijsem.0.004332

Prüss-Ustün, A., Wolf, J., Bartram, J., Clasen, T., Colford, J. M., Freeman, M. C., Gordon, B., Hunter, P. R., Medlicott, K., Neira, M., Stocks, M., and Johnston, R. B. (2019). Burden of disease from inadequate water, sanitation and hygiene for selected adverse health outcomes: An updated meta-analysis. *Environmental Health,* 18(1): 1–15. https://doi.org/10.1186/s12940-019-0502-6

Serwaa, D., Lamptey, E., Asante-Poku, A., Asamoah-Akuoko, L., and Baryeh, K. (2020). Microbiological quality of water sources in sub-Saharan Africa: A systematic review. *Water Science and Technology,* 82(6): 1101–1113. https://doi.org/10.2166/wst.2020.367

Sgroi, M., Pelosi, M., Pryor, M., Nakamura, M., and Muñoz, J. F. (2021). Occurrence of disinfection by-products in wastewater treatment plants: A global overview. *Chemosphere,* 285: 131423. https://doi.org/10.1016/j.chemosphere.2021.131423

Shaikh, S., Yaqoob, M., and Agwan, M. A. (2023). Phytochemical-nanoparticle conjugates as antibacterial agents: Recent advances and mechanisms of action. *Nanomedicine: Nanotechnology, Biology and Medicine,* 49: 102657. https://doi.org/10.1016/j.nano.2023.102657

Van Boeckel, T. P., Pires, J., Silvester, R., Zhao, C., Song, J., Criscuolo, N. G., Gilbert, M., Bonhoeffer, S., and Laxminarayan, R. (2019). Global trends in antimicrobial resistance in animals in low- and middle-income countries. *Science,* 365(6459): eaaw1944. https://doi.org/10.1126/science.aaw1944

Zugaro, S., Benedetti, E., and Caioni, G. (2023). Garlic (*Allium sativum*) as an ally in the treatment of inflammatory bowel diseases. *Current Issues in Molecular Biology,* 45(1): 685–698. https://doi.org/10.3390/cimb45010046 .

Funding
Not applicable.

Institutional Review Board Statement
Not applicable.

Informed Consent Statement
Not applicable.

Acknowledgements
The authors thank Bello M.A., and Afolabi M.A. of the Department of Microbiology and Biotechnology, Ajayi Crowther University, for their support during the research.

Conflict of Interest
The author declared no conflict of interest in the manuscript.

Authors' Declaration
The author(s) hereby declare that the work presented in this article is original and that they will bear any liability for claims relating to the content of this article.

Author Contributions
Conceptualisation: OAA. Laboratory work: OAA and TEL. Statistical analysis: OAA, TEL, and BMP. Original draft, Writing, Review and Editing: OAA, TEL, BMP. All authors approved the final manuscript

Cite article as:

Adeyemi, O. A., Lawal, T. E. & Popoola, B. M. (2026). Combinatorial Antibacterial Activity of Allium sativum (Garlic) with Titanium Dioxide (TiO_2) and Zinc Oxide (ZnO) Nanoparticles against Selected Bacterial Isolates from a University Hostel Wastewater in Oyo, Nigeria. *Ajayi Crowther Journal of Pure and Applied Sciences, 5*(2), 30–46. https://doi.org/10.56534/acjpas.v5i2.198